3D Aortic Motion Estimation for Image-Guided Intervention

R. E. Clough[1], C. Buerger[1], C. Kolbitsch[1], M. Henningsson[1], P. Taylor[1], C. Prieto[1], and T. Schaeffter[1]
[1]Division of Imaging Sciences and Biomedical Engineering, King's College London, Westminster Bridge Road, London, United Kingdom

INTRODUCTION: Endovascular repair is now the method of choice for treatment of thoracic aortic disease. [1] State-of-the-art arch devices allow antegrade perfusion of the brain by cannulation and insertion of a stent in each of the individual branches. Much of the complexity of the procedure is related to the anatomy of the aortic arch and the consequent challenges in accurate catheter navigation and device placement [2]. X-ray fused with MRI (XMR) integrates 3-D anatomy information from MRI (roadmap) with x-ray angiography and by providing enhanced image guidance, is associated with increased procedure efficacy and reduce radiation exposure. [3-5]. To increase the fidelity of these roadmaps physiological cardiac and respiratory motion must be incorporated. However, an assessment of the 3-D aortic motion has not previously been described. In this work we quantify the 3D deformation of the aorta caused by both cardiac and respiratory motion and evaluate the accuracy of both affine and non-rigid motion corrections.

METHODS: Imaging studies were performed in five healthy volunteers on a 1.5T MRI scanner (Philips Healthcare, Best, Netherlands) with a 32-channel coil. 3D cardiac cine images were acquired under breath-hold with ECG gating using an angulated slab covering the aorta. A balanced FFE sequence was used with FOV=320x270x50mm; acquired resolution=3x3x3mm; SENSE-factor=2; TR/TE=2.9/1.4ms; FA=60°; T2prep (TE=50ms); half-scan-y=0.625; 25 cardiac phases.
Respiratory resolved data was acquired in a single cardiac phase (subject-specific mid-diastolic trigger delay) using a free-breathing 3D balanced SSFP sequence FOV=288x288x288mm; resolution =3x3x3mm; TR/TE=4.3/2.2ms; cardiac acquisition window =100ms; FA=90°; T2prep (TE=50ms); fat sat (SPIR); SENSE factor = 6. Data was retrospectively assigned to different respiratory positions in a 3mm gating window.

A 3D surface rendered roadmap of the aorta (shown in Fig 1a) was obtained by manual segmentation of both cardiac and respiratory acquisitions. The 3D deformation of the aorta was quantified for affine and non-rigid descriptions by applying an intensity-based image registration [6]. The accuracy of both cardiac and respiratory motion estimations was validated by computing target registration errors TRE_A (affine) and TRE_{NR} (non-rigid) for manually defined landmarks.
Thirty-six clinically relevant points along the aorta were defined and clustered into three groups: (i) ascending aorta; (ii) aortic arch, and (iii) descending thoracic aorta (Fig 1a). The 3D mean displacement of each cluster over time was analyzed in foot-head (FH), anterior-posterior (AP) and right-left (RL) directions for both respiratory and cardiac motion.

RESULTS: The maximum aortic displacement caused by cardiac and respiratory motion was 17mm and 8mm respectively (Fig 2). The mean displacement between the landmarks in the first image and their corresponding position in the following frames was 2.81±1.91mm due to respiratory motion and 3.91±4.03mm due to cardiac motion.
Affine respiratory motion registrations contained translation, scaling and shear components and showed a similar accuracy to non-rigid registration (TRE_A = 1.52±0.69mm and TRE_{NR} = 1.52±0.77mm). However, affine registration was unable to correct for cardiac motion and a significantly higher accuracy was achieved using the non-rigid algorithm (TRE_A = 3.72±3.83mm and TRE_{NR} = 1.95±1.22mm) (Fig 2).
The average non-rigid displacement of the aorta caused by cardiac and respiratory motion is shown in Fig 1. Foot-head, RL and AP motion is displayed for each cluster over time with maximum displacements observed at end-systole (time =10) and end-inspiration (time = 7). The maximum non-rigid aortic displacements due to cardiac and respiratory motion in AP, RL and FH directions are shown for each cluster in Fig 3. For both cardiac and respiratory motion the predominant direction of displacement was FH in all sections of the aorta. Cardiac motion resulted in a greater amount of RL and AP displacement compared with respiratory motion, especially in the ascending aorta.

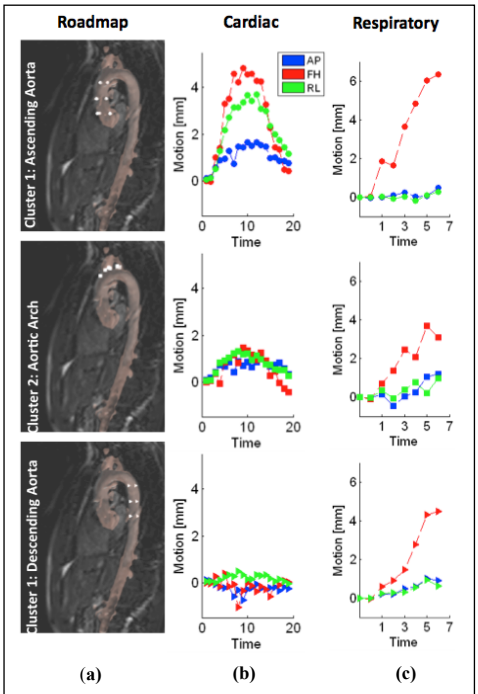

***Fig 1**: (a) Road map and clusters (1. ascending aorta, 2. aortic arch and 3. Descending aorta); (b) Estimated deformation over one cardiac cycle (time 1-20) averaged over all volunteers; and (c) over one respiratory cycle (time 1-7) for a single volunteer. We show the results for one volunteer due to the different number of respiratory phases between individuals.*

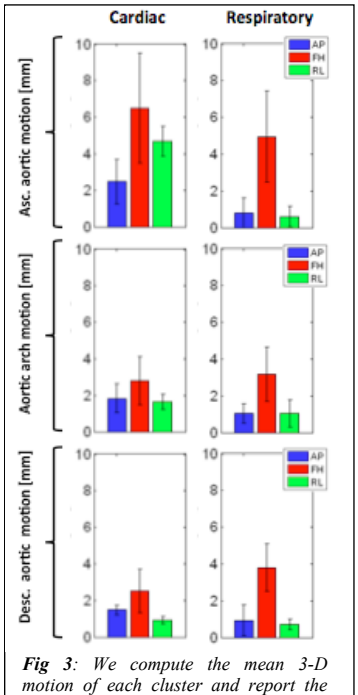

***Fig 3**: We compute the mean 3-D motion of each cluster and report the maximum observed deformation averaged over all volunteers. Foot-head was the predominant motion component for both cardiac and respiratory cases although greater amounts of RL and AP displacement were seen with cardiac motion.*

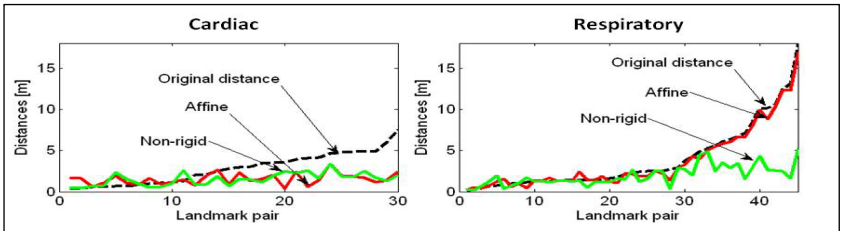

***Fig 2**: Absolute aortic displacement over all landmarks for all volunteers. For illustration the displacements are sorted from small (left) to large (right). Similar accuracy for respiratory motion estimation was achieved for both registration techniques whereas a significantly higher accuracy was achieved by non-rigid registration for cardiac motion even for large displacements.*

CONCLUSIONS: We have shown that there is significant 3D displacement of the aorta as a result of both cardiac and respiratory motion. Respiratory motion can be adequately described by a simple affine registration but a non-rigid registration is required for the complex deformation caused by cardiac motion. The magnitude of aortic displacement seen in this study was up to two-fold the diameter of branch vessel lumens and in some instances, as large as the diameter of the aorta itself. This novel technique has the potential to deliver a patient-specific method to assess changes in aortic deformation and could provide important information required for complex aortic interventions.

REFERENCES: [1] Coady MA, Circ 2010 [2] Carrell TW, JEVT 2010 [3] Rezavi R, Lancet 2003 [4] King AP, Medical Image Analysis, 2009 [5] Rhode KS, IEEE 2005 [6] Buerger C, ISBI 2010.